Novel di-2-pyridyl–derived iron chelators with marked and selective antitumor activity: in vitro and in vivo assessment

Jun Yuan, David B. Lovejoy, and Des R. Richardson

Aroylhydrazone and thiosemicarbazone iron (Fe) chelators have potent antitumor activity. The aim of the current study was to examine the antitumor effects and mechanisms of action of a novel series of Fe chelators, the di-2-pyridyl thiosemicarbazones. Of 7 new chelators synthesized, 4 showed pronounced antiproliferative effects. The most active chelator was Dp44mT, which had marked and selective antitumor activity—for example, an IC_{50} of 0.03 μM in neuroepithelioma cells compared with more than 25 μM in mortal fibroblasts. Indeed, this antiproliferative activity was the greatest yet observed for an Fe chelator. Efficacy was greater than it was for the cytotoxic ligand 311 and comparable to that of the antitumor agent doxorubicin. Strikingly, Dp44mT significantly ($P < .01$) decreased tumor weight in mice to 47% of the weight in the control after only 5 days, whereas there was no marked change in animal weight or hematologic indices. Terminal deoxyribonucleotidyl transferase (TdT)–mediated dUTP nick end-labeling (TUNEL) staining demonstrated apoptosis in tumors taken from mice treated with Dp44mT. This chelator caused a marked increase of caspase-3 activity in murine Madison-109 (M109) cells. Caspase activation was at least partially mediated by the release of mitochondrial holo-cytochrome *c* (h-cytc) after incubation with Dp44mT. In conclusion, Dp44mT is a novel, highly effective antitumor agent in vitro and in vivo that induces apoptosis. (Blood. 2004;104: 1450-1458)

Introduction

Iron (Fe) is essential for proliferation, and many studies have shown that tumor cells are more sensitive to Fe deprivation than normal cells.[1-11] This sensitivity probably exists because cancer cells have greater Fe requirements than their normal counterparts[12-15] and because cancer cells express higher levels of the Fe-containing enzyme, ribonucleotide reductase (RR), which is the critical rate-limiting step in DNA synthesis.[16-21]

Many in vitro[2,4,7-9,21-28] and in vivo[6,29,30] studies and clinical trials[3,5,31-36] have demonstrated that chelators are effective antiproliferative agents (for reviews, see Hershko,[10] Lovejoy and Richardson,[11] and Richardson[37]). The most well-studied chelator is desferrioxamine (DFO; Figure 1).[10,11] However, its short half-life and low efficacy at permeating membranes limit its antiproliferative activity.[22,38] Indeed, these factors probably resulted in its failure to inhibit tumor growth in some studies.[39,40] One group of ligands with high Fe chelation efficacy is the pyridoxal isonicotinoyl hydrazone (PIH) class.[41-44] We characterized PIH analogs that show far greater Fe chelation efficacy and antiproliferative activity than DFO.[23,24,45] Some of these ligands, such as 2-hydroxy-1-naphthylaldehyde isonicotinoyl hydrazone (311; Figure 1) inhibit RR activity[9] and affect the expression of molecules vital for cell cycle control.[46-48] One mechanism by which chelators and other factors (eg, oxidative stress) cause tumor cell death may be through the induction of apoptosis.[22,24,49-56] However, the precise mechanisms involved in chelator-mediated apoptosis remain unclear, particularly for aroylhydrazone ligands.

The caspase enzymes are common executors of apoptosis.[52,57,58] Two caspase-activating cascades that regulate apoptosis have been described; one is initiated through death receptors (eg, CD95), and the other is triggered by changes in mitochondrial integrity.[52,59,60] In the former, engaging death receptors by their ligands (eg, CD95L) leads to the formation of a death-inducing signaling complex.[52] Activated death receptors recruit and activate caspase-8, which initiates executioner caspases, including caspase-3. In mitochondrial-dependent apoptosis, the release of holo-cytochrome *c* (h-cytc) into the cytosol results in the formation of an apoptosome containing h-cytc, Apaf-1, and procaspase-9.[52,57] In the apoptosome, procaspase-9 becomes activated and triggers executioner caspases that initiate terminal events overlapping with those induced by the death receptor pathway.[52,57] Major modulators of the mitochondrial pathway of apoptosis include the *Bcl-2/Bax* gene family.[52,61,62] The Bcl-2 group of proteins is found in the outer mitochondrial membrane and plays a role in its stability.[52,61] In contrast, the Bax proteins are cytosolic molecules that, on receipt of an apoptotic signal, migrate to the mitochondrion binding to the permeability transition pore.[52,62] Imbalance of Bcl-2 and Bax induces the loss of selective ion permeability resulting in h-cytc release, which initiates the caspase cascade responsible for apoptosis.[52,53,62] If chelators cause tumor cell death by engaging the apoptotic pathway, then inducting apoptosis becomes a vital aim.

Previously, we characterized the in vitro antiproliferative activity of hybrid Fe chelators derived from aroylhydrazones and

From the Iron Metabolism and Chelation Program, Children's Cancer Institute Australia for Medical Research, Randwick, Sydney, Australia.

Submitted March 9, 2004; accepted April 12, 2004. Prepublished online as *Blood* First Edition Paper, May 18, 2004; DOI 10.1182/blood-2004-03-0868.

Supported by a fellowship and a project grant from the National Health and Medical Research Council of Australia.

J.Y. and D.B.L. contributed equally to this study.

Reprints: Des R. Richardson, Iron Metabolism and Chelation Program, Children's Cancer Institute Australia for Medical Research, PO Box 81, High St, Randwick, Sydney, NSW, 2031, Australia; e-mail: d.richardson@ccia.org.au.

The publication costs of this article were defrayed in part by page charge payment. Therefore, and solely to indicate this fact, this article is hereby marked "advertisement" in accordance with 18 U.S.C. section 1734.

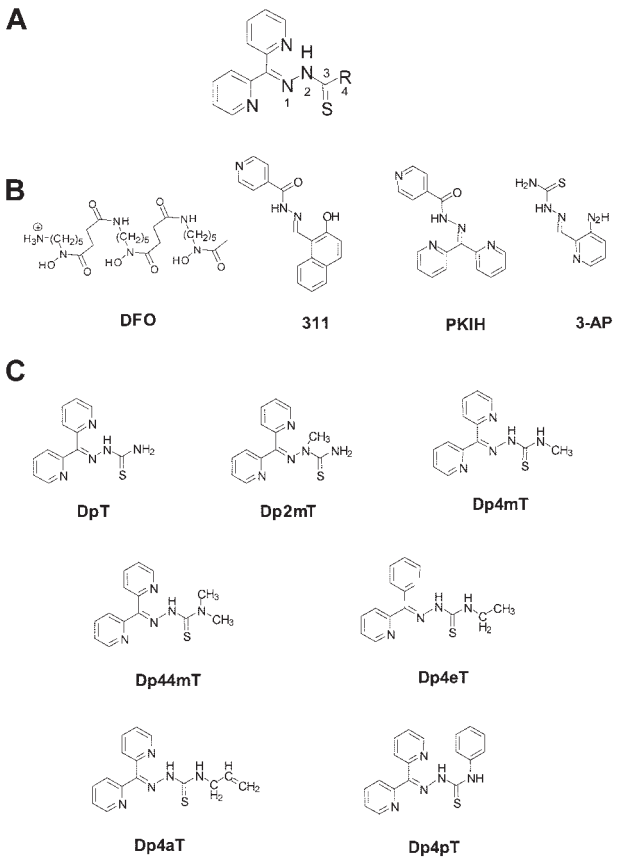

Figure 1. Structural formulas of the Fe chelators described in this study. (A) General structure of the DpT analogs showing the numbering scheme used. (B) Structures of DFO, 311, 3-AP, and PKIH. (C) Structures of DpT, Dp2mT, Dp4mT, Dp44mT, Dp4eT, Dp4aT, and Dp4pT.

thiosemicarbazones.[6,7,23,24,63] Recently, we discovered that the di-2-pyridyl moiety results in pronounced antitumor activity of aroylhydrazones (eg, di-2-pyridylketone isonicotinoyl hydrazone [PKIH]; Figure 1).[8] Therefore, it was important to condense di-2-pyridyl with a range of thiosemicarbazides to derive a new group of Fe chelators, the di-2-pyridyl thiosemicarbazone (DpT) analogs (Figure 1).

Our investigation demonstrated that novel DpT analogs, in particular di-2-pyridylketone-4,4,-dimethyl-3-thiosemicarbazone (Dp44mT; Figure 1), showed selective antitumor activity. In addition, Dp44mT strikingly decreased tumor growth in mice while not markedly affecting animal weight or a range of hematologic indices. This chelator also induced tumor cell apoptosis that was at least partially mediated through the release of mitochondrial h-cytc into the cytosol and the activation of caspase-3, -8, and -9. The release of h-cytc could be mediated by the imbalance of Bcl-2 and Bax expression induced by incubation of cells with Dp44mT.

Materials and methods

Chelators

DpT analogs and 311 were prepared using standard procedures.[8,64,65] DFO was obtained from Novartis (Basel, Switzerland). 3-AP (Triapine; 3-aminopyridine-2-carboxaldehyde thiosemicarbazone) was a gift from Vion Pharmaceuticals (New Haven, CT).

Antibodies

Rabbit antiactive caspase-3 antibody, rabbit antiactive caspase-8 antibody, and Annexin V–fluorescein isothiocyanate (FITC) were from BD PharMingen (San Diego, CA). Anti–h-cytc monoclonal antibody (mAb) was from R&D Systems (Minneapolis, MN). Rabbit antiactive caspase-9 antibody, mouse anti–Bcl-2, and mouse anti-Bax antibodies were obtained from Santa Cruz Biotechnology (Santa Cruz, CA). Antimouse β-actin antibody, horseradish peroxidase–conjugated antirabbit, and antimouse immunoglobulin G (IgG) were from Sigma Chemical (St Louis, MO).

Cell culture

Human MRC-5 fibroblasts, SK-N-MC neuroepithelioma cells, SK-Mel-28 melanoma cells, and MCF-7 breast cancer cells were obtained from the American Type Culture Collection (Rockville, MD). The murine Madison-109 (M109) lung cancer cell type was obtained from the National Cancer Institute (Fredrick, MD). Cells were grown as described previously.[13]

Labeling of transferrin with ^{59}Fe

Apotransferrin (Sigma) was labeled with iron Fe 59 (^{59}Fe; Dupont-NEN, Boston, MA) to produce ^{59}Fe-transferrin (^{59}Fe-Tf) using standard procedures.[13,14]

Effect of chelators on cellular proliferation

The effect of the chelators on proliferation was examined using the MTT assay.[23]

Iron uptake and iron efflux assays

The effect of chelators on cellular ^{59}Fe efflux and reducing ^{59}Fe uptake from ^{59}Fe-Tf by cells was studied using standard procedures.[22-24]

Determining the maximum tolerated dose in CD_2F_1 hybrid mice

BALB/c and DBA/2 mice were crossed to produce CD_2F_1 animals (procedures approved by the Animal Ethics Committee, University of New South Wales, Australia). Groups of 8 female CD_2F_1 mice (8-10 weeks old) were fed and watered ad libitum and were injected through the tail vein with the chelators in 30% propylene glycol in 0.9% sterile saline, twice a day, 6 hours apart, 5 days a week for 2 weeks.[40] The maximum tolerated dose (MTD) was defined as the dose at which 30% of a cohort was killed because of markedly deteriorating health or lost weight in excess of 10%.[40]

Inhibition of M109 lung cancer cell growth by iron chelators in vivo

CD_2F_1 mice were subcutaneously implanted with 1×10^5 M109 cells.[6] Dp44mT was dissolved in propylene glycol, as described above. An established protocol[6] was used to test antitumor activity of the chelators in the M109 cancer model. Four days after engraftment, the tumors were palpable and the ligands were administered intravenously, twice a day for 5 days, followed by a rest period of 2 days when the animal was not injected.[6] On the 12th day after tumor implantation, mice were killed using methoxyflurane, and blood was obtained by cardiac puncture. Blood indices were measured using a Sysmex Blood Counter (Prince of Wales Hospital, Sydney, Australia). Mouse body weight changes during the treatment period were recorded. The tumor grew subcutaneously as a well-circumscribed mass surrounded by fibrous membranes and was simple to excise. Tumors were weighed and fixed for histologic examination. Experimental groups consisted of 8 mice for the control and each treatment. 3-AP (Vion Pharmaceuticals) was used as antitumor agent control because it is a chelator with potent antitumor activity with a mechanism of action similar to that of the chelators under investigation (ie, it binds Fe).[6,34,35]

In situ end labeling of fragmented DNA assay

DNA cleavage was assessed using the terminal deoxyribonucleotidyl transferase (TdT)–mediated dUTP nick end-labeling (TUNEL) reaction.[67,68]

Apoptosis assay using flow cytometry

Apoptotic cells were detected using a flow cytometer (FACSCalibur; Becton Dickinson, San Jose, CA) with fluorescein isothiocyanate (FITC)–labeled Annexin V (BD PharMingen) binding to translocated plasma membrane phosphatidylserine (PS).[69] Propidium iodide (PI) was added to identify loss of integrity, which is indicative of necrotic and late-stage apoptotic cells.[69]

Preparation of cytosolic and stromal-mitochondrial membrane fractions and Western blot analysis

Cytosolic and stromal-mitochondrial membrane (SMM) fractions and Western blotting were prepared using standard techniques.[46,70]

Caspase activation and activity assay

Cultured M109 cells were treated with or without Dp44mT (1 μM) for 0 to 48 hours at 37°C. Cells were lysed,[70] and caspase activities were determined using the BD Apolert Caspase Assay Plate (BD Biosciences, San Diego, CA). Cell-permeable pancaspase-3, -8, and -9 inhibitors (BD Biosciences) were included as inhibitory controls.

Intracellular reactive oxygen species assay

Intracellular reactive oxygen species (ROS) generation was assessed using 2′,7′-dichloro-fluorescein-diacetate (H_2DCF-DA; Sigma).[71] H_2DCF-DA diffuses into cells, where it is hydrolyzed to the nonfluorescent derivative H_2DCF, which is trapped within cells. H_2DCF becomes highly fluorescent when oxidized by O_2^-, H_2O_2, or HO−.[71] Cellular fluorescence intensity is directly proportional to intracellular ROS.[71] M109 cells (1×10^5 cells/well) were incubated with or without 1 μM Dp44mT for 0 to 48 hours or 50 μM H_2O_2 (positive control)[71] for 10 minutes at 37°C. Cells were then incubated with H_2DCF-DA (5 μM) for 20 minutes at 37°C and washed twice.[71] The fluorescence of oxidized DCF in cells was measured using flow cytometry.[71]

Statistical analysis

All values are expressed as mean ± SEM of 3 experiments. Statistical analysis was performed using the Student *t* test. Results were considered statistically significant when *P* values were lower than .05.

Results

Effect of the DpT analogs on the proliferation of neoplastic cells

Initially, the ability of the DpT analogs to inhibit proliferation was assessed using SK-N-MC neuroepithelioma cells (Table 1) because the effect of chelators on their growth is well characterized.[7,23,24,45] Our studies identified Dp44mT, Dp4eT, Dp4aT, and Dp4pT as having very high antiproliferative activity (IC_{50}, 0.03-0.06 μM; Table 1). These ligands were significantly ($P < .0001$) more active than DFO (IC_{50}, 5 μM) and have greater efficacy than other potent Fe chelators assessed in our laboratory, namely 311 (IC_{50}, 0.3 μM; Table 1). Adding Fe to these DpT analogs to form their complexes did not significantly affect antiproliferative activity, indicating a possible role for the Fe complexes in their cytotoxic effects. Compared with the antiproliferative activity of the established cytotoxic agent, doxorubicin, in SK-N-MC cells (IC_{50}, 0.02 μM; Table 1), Dp44mT, Dp4eT, Dp4aT, and Dp4pT had similar efficacy. The chelator 3-AP (Figure 1B), which is undergoing clinical trials as an antitumor agent,[34,35] had less activity (IC_{50}, 0.26 μM; Table 1) than these latter DpT analogs. Dp4mT also demonstrated appreciable activity against SK-N-MC cells and was comparable to 3-AP with an IC_{50} value of 0.19 μM (Table 1).

Table 1. IC_{50} values in neoplastic and normal cells

	Neoplastic cells			Normal cells
	SK-N-MC neuroepithelioma	SK-Mel-28 melanoma	MCF-7 breast cancer	MRC-5 fibroblasts
DFO	5 ± 2	15 ± 7	14 ± 9	> 25
311	0.3 ± 0.2	0.9 ± 0.5	—	> 25
DpT	> 25	> 25	> 25	> 25
Dp2mT	> 25	> 25	> 25	> 25
Dp4mT	0.19 ± 0.1	0.6 ± 0.5	0.3 ± 0.2	> 25
Dp44mT	0.03 ± 0.01	0.06 ± 0.03	0.06 ± 0.01	> 25
Dp4eT	0.06 ± 0.01	0.09 ± 0.06	0.08 ± 0.01	> 25
Dp4aT	0.06 ± 0.01	0.10 ± 0.06	0.07 ± 0.01	> 25
Dp4pT	0.05 ± 0.006	0.09 ± 0.05	0.07 ± 0.01	> 25
3-AP	0.26 ± 0.01	2.6 ± 0.6	3.0 ± 1.5	—
Doxorubicin	0.02 ± 0.01	0.35 ± 0.09	0.6 ± 0.2	—

Each IC_{50} value (given in μM) is the mean ± SEM of at least 3 experiments performed. Cells were incubated in the presence and absence of DFO, 311, 3-aminopyridine-2-carboxaldehyde thiosemicarbazone, doxorubicin, and the DpT series of chelators (0-25 μM) for 72 hours at 37°C. After this incubation period, cellular proliferation was determined by the MTT assay.[23] — indicates not determined.

In contrast to the most active DpT analogs described above, the parent compound of this series, DpT (Figure 1), showed little activity against SK-N-MC cells; the IC_{50} value was greater than 25 μM (Table 1). Similarly, the Dp2mT analog also demonstrated low activity, probably because the 2-methyl group (Figure 1A,C) prevented electron delocalization and metal ion binding. Hence, Dp2mT served as a negative control, demonstrating that at least part of the antiproliferative effect of these chelators was attributed to metal binding.

To investigate the spectrum of antineoplastic activity, the DpT analogs were assessed against the SK-Mel-28 melanoma and the MCF-7 breast cancer cell lines (Table 1). All the DpT analogs, apart from DpT and Dp2mT, were far more active ($P < .0001$) than DFO at inhibiting the proliferation of SK-Mel-28 melanoma and MCF-7 breast cancer cells (Table 1). Against these cell lines, Dp44mT, Dp4eT, Dp4aT, and Dp4pT were the most active (IC_{50}, 0.06-0.10 μM; Table 1). Dp44mT was the most effective antiproliferative agent when assessing all tumor cell lines. Dp4mT was less active against these cell types than the latter DpT analogs (IC_{50}, 0.3-0.6 μM; Table 1). Again, DpT and Dp2mT showed little activity against SK-Mel-28 melanoma cells and MCF-7 breast cancer cells (IC_{50} greater than 25 μM).

Chelators have less effect on the proliferation of normal cells than neoplastic cells

Clinically useful antitumor agents have little effect on normal cells while inhibiting neoplastic cell growth. Hence, it was important to compare the antiproliferative effects of the active DpT series chelators between neoplastic and normal cells (Figure 2; Table 1). In contrast to the marked antiproliferative activity of Dp44mT, Dp4eT, Dp4aT, and Dp4pT against immortal neoplastic cells, these chelators had relatively little effect on the proliferation of mortal MRC-5 fibroblasts; IC_{50} values were greater than 25 μM (Figure 2;

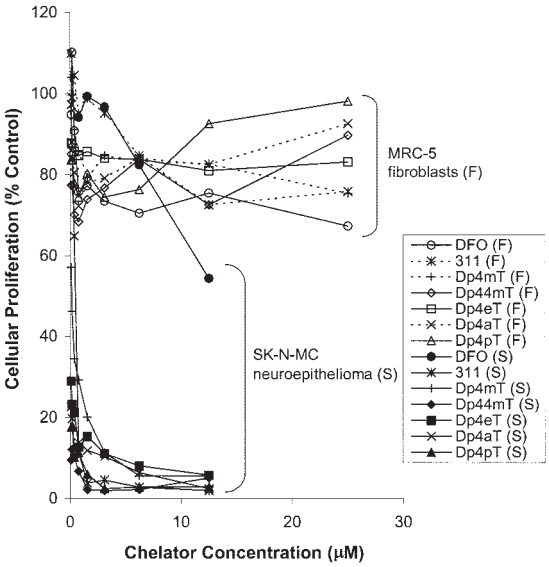

Figure 2. The most effective DpT analogs and 311 (internal control) show selective antiproliferative activity against immortal SK-N-MC neuroepithelioma cells (S) compared with mortal MRC-5 fibroblasts (F). Cells were incubated in the presence or absence of the chelators (0-25 μM) for 72 hours at 37°C.[23] After this incubation period, cellular density was measured using the MTT assay. Cellular proliferation was expressed as a percentage of that found for the untreated cells. Each data point represents the mean of 2 replicates in a typical experiment of at least 3 to 5 experiments.

Table 1). The difference in the antiproliferative effect shown in Figure 2 may be attributed to the slower proliferation of MRC-5 fibroblasts (doubling time, 22 hours) compared with SK-N-MC cells (doubling time, 16 hours).[7]

Effect of the DpT analogs on iron efflux from SK-N-MC cells

To determine the possible role of Fe chelation efficacy in the antiproliferative activity of the DpT analogs, we examined the ability of the ligands to directly mobilize ^{59}Fe from SK-N-MC cells (Figure 3A). Cells were prelabeled for 3 hours at 37°C with ^{59}Fe-Tf (0.75 μM), washed, and then reincubated for 3 hours at 37°C with the chelators (25 μM; Figure 3A). As standards, DFO and 311 were used, as their activities are well characterized.[7-9,22-24]

Broadly, the ligands can be grouped into 2 classes depending on their ability to mobilize cellular ^{59}Fe. The first group had very low activity and included DpT and Dp2mT, which caused the efflux of 6% to 7% of total cellular ^{59}Fe, whereas control cells reincubated with media alone released 5% of ^{59}Fe (Figure 3A). These data correlate with the small effect of these chelators on the inhibition of tumor cell growth (Table 1). As shown previously,[7-9,22-24] DFO only resulted in the mobilization of 14% of cellular ^{59}Fe (Figure 3A).

The second group consisted of the remaining DpT analogs, which were significantly ($P < .0001$) more effective than DFO at mobilizing ^{59}Fe and resulted in the release of 37% to 47% of cellular ^{59}Fe (Figure 3A). Trypan blue staining and phase-contrast microscopy demonstrated that the increased ^{59}Fe release was not caused by a decrease in cellular viability over the 3-hour incubation with the chelator. Dp44mT was the most efficient DpT analog assessed, resulting in the release of 47% of ^{59}Fe and having an efficacy similar to that of the potent ligand 311[7-9] (Figure 3A). The high efficacy of this second group of DpT analogs at inducing ^{59}Fe efflux correlated with their antitumor activity (Table 1).

Effect of the chelators on iron uptake from transferrin by SK-N-MC neuroepithelioma cells

To further characterize the effects of the chelators on Fe metabolism, we examined their ability to inhibit ^{59}Fe uptake from ^{59}Fe-Tf (0.75 μM) by SK-N-MC cells in the absence or presence of the chelators (25 μM) for 3 hours at 37°C (Figure 3B). DpT and Dp2mT had little effect on preventing ^{59}Fe uptake (Figure 3B). The most efficient chelators, 311 and Dp44mT, limited ^{59}Fe uptake to 5% to 9% of the control, and their activity was greater ($P < .0001$) than that of DFO (Figure 3B). These results agree with the ability of these ligands to mobilize cellular ^{59}Fe (Figure 3A). All DpT analogs (except DpT and Dp2mT) show much greater efficacy than DFO in preventing ^{59}Fe uptake from ^{59}Fe-Tf by cells (Figure 3B).

Effects of Dp44mT on iron uptake from Tf and iron mobilization from M109 cells

These experiments and our previous work suggested that of all chelators assessed in our laboratory,[7-9,23,24] Dp44mT showed the most promise for in vivo evaluation. Further studies aimed to assess the ability of this chelator to inhibit the growth of M109 lung carcinoma cells in mice. This model was chosen because the tumor is refractory to cytotoxic drugs and has been used to assess the activity of the chelator 3-AP.[6]

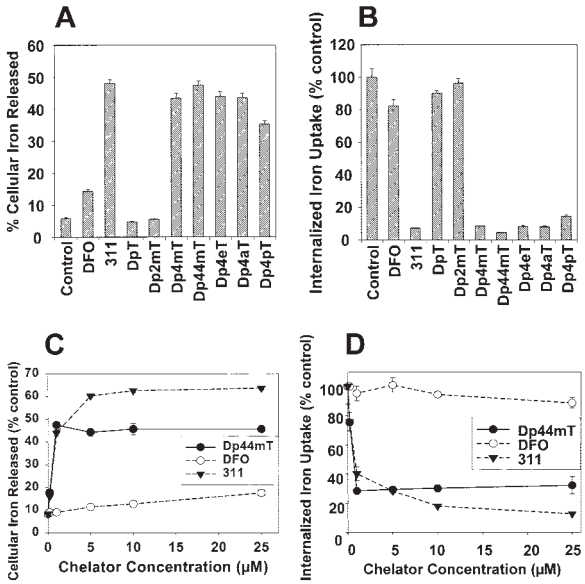

Figure 3. Effect of the DpT analogs compared with DFO and 311 on ^{59}Fe mobilization and cellular ^{59}Fe uptake from ^{59}Fe-Tf in SK-N-MC neuroepithelioma and M109 cells. (A) Effect of chelators on ^{59}Fe mobilization from prelabeled SK-N-MC neuroepithelioma cells. Cells were prelabeled with ^{59}Fe-Tf (0.75 μM) for 3 hours at 37°C, washed, and then reincubated for 3 hours at 37°C in the presence of medium alone (control) or medium containing the chelators (25 μM). (B) Effect of the chelators at preventing ^{59}Fe uptake from ^{59}Fe-Tf by SK-N-MC cells. Cells were incubated for 3 hours at 37°C in media containing either ^{59}Fe-Tf (0.75 μM) alone (control) or ^{59}Fe-Tf (0.75 μM) and the chelators (25 μM). After this incubation, the cells were washed and incubated with pronase (1 mg/mL) for 30 minutes at 4°C to measure internalized ^{59}Fe.[13,14] (C) Effect of the chelators on ^{59}Fe mobilization from prelabeled M109 cells as a function of chelator concentration. M109 cells were prelabeled as described for panel A, then reincubated with the chelator (0.2-25 μM) for 3 hours at 37°C. (D) Effect of the chelators at preventing ^{59}Fe uptake from ^{59}Fe-Tf by M109 cells as a function of chelator concentration. M109 cells were incubated with ^{59}Fe-Tf (0.75 μM) in the presence of the chelators (0.2-25 μM) for 3 hours at 37°C. Cells were washed and incubated with pronase as described for panel B. Results are expressed as the mean ± SD of 3 replicates in a typical experiment of 3 performed.

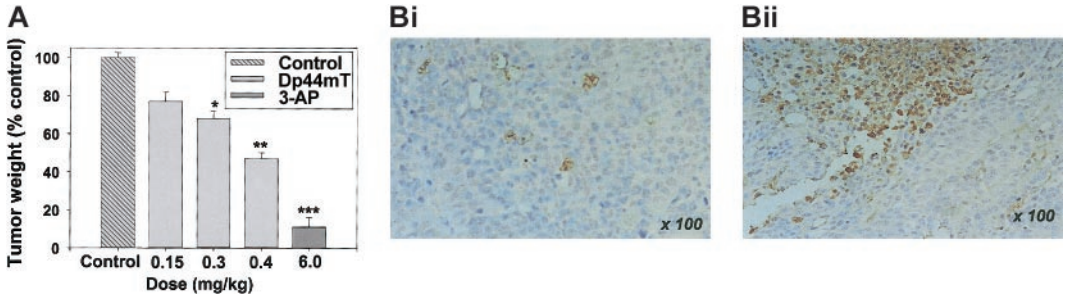

Figure 4. Dose-dependent inhibition of M109 lung carcinoma growth in mice by Dp44mT and 3-AP. (A) Dp44mT and, to a greater extent, 3-AP markedly decreased the growth of M109 lung carcinoma in mice after a 5-day treatment regimen. (B) Induction of apoptosis in tumors after injection of (i) vehicle control or (ii) Dp44mT, as determined using TUNEL assay. (A) 1×10^5 M109 cells were subcutaneously implanted in CD2F1 mice. The chelators Dp44mT and 3-AP were injected intravenously twice daily for 5 consecutive days starting on the fourth day after tumor implantation. Tumor weight was measured on the 12th day after implantation. n = 8 in each experimental group. Data were analyzed using the Student *t* test. *$P < .05$ compared with control. **$P < .01$ compared with control. ***$P < .0001$. (B) M109 lung carcinoma specimens from mice treated as for panel A with (i) vehicle control or (ii) Dp44mT were fixed in 10% (vol/vol) buffered formalin and embedded in paraffin. Sections were stained for apoptotic cells in situ using the TUNEL assay. Positive nuclei stained brown, and negative nuclei stained blue. Results in panel A are mean ± SEM for 3 experiments, whereas data in panel B are typical of results found in 3 separate experiments.

Initial studies were performed using M109 carcinoma cells in culture to determine the effect of Dp44mT on mobilizing intracellular ^{59}Fe (Figure 3C) and inhibiting ^{59}Fe uptake from ^{59}Fe-Tf (Figure 3D). Again, as controls, cells were incubated with DFO and 311.[23,24,45] The effect of ligand concentration on increasing ^{59}Fe mobilization was examined by labeling M109 cells with ^{59}Fe-Tf (0.75 μM) for 3 hours at 37°C followed by washing and reincubation with the chelators (0.2-25 μM) for 3 hours at 37°C (Figure 3C). DFO was the least effective ligand examined, and at 25 μM it released only 12% ± 1% ^{59}Fe, whereas control medium released 8% ± 1% (Figure 3C). In contrast, 311 increased cellular ^{59}Fe release from 8% ± 1% (control medium) to 60% ± 1% at 5 μM (Figure 3C). Dp44mT was slightly less effective than 311; at 1 μM, ^{59}Fe release plateaued, resulting in the efflux of 48% ± 2% of ^{59}Fe (Figure 3C).

The most active compound for inhibiting ^{59}Fe uptake by M109 cells was 311 (Figure 3D). At 1 μM, 311 reduced ^{59}Fe uptake to 40% ± 4% of the control. In contrast, DFO had little effect. The activity of Dp44mT was similar to that of 311 up to 5 μM, where it reduced ^{59}Fe uptake to 30% ± 1% of the control (Figure 3D). At higher concentrations, up to 25 μM, 311 was more effective than Dp44mT. These studies (Figures 2 and 3) and the marked antiproliferative activity of Dp44mT (Figure 2; Table 1) demonstrated that it was a potent antitumor agent.

Dose-dependent inhibition of M109 lung carcinoma in mice

In control mice, the M109 tumor grew rapidly. In fact, 7 days after engraftment, the tumor wet weight was approximately 0.1 g, and this increased after 14 days to approximately 1 g. Figure 4A shows the effects of 0.15, 0.3, and 0.4 mg/kg Dp44mT (MTD, 0.4 mg/kg) on tumor growth after intravenous injection twice daily for 5 consecutive days. As a relevant positive control, animals were administered 3-AP at its MTD (6 mg/kg). Dp44mT inhibited tumor growth in a dose-dependent manner (Figure 4A). At 0.4 mg/kg, it reduced tumor weight to 47% ($P < .01$) of control values (control tumor weight, 0.48 ± 0.08 g). 3-AP was markedly more effective than Dp44mT, significantly ($P < .001$) reducing tumor weight to 10% of the control (Figure 4A).

No significant differences occurred in weight loss or leukocyte cell count in the control mice compared with mice treated with Dp44mT (Table 2). However, compared with the control group, slight ($P < .05$) decreases in hemoglobin level, hematocrit, erythrocyte count, and platelet count were observed in animals treated with Dp44mT at its MTD (0.4 mg/kg) but not at lower doses (Table 2). Interestingly, Dp44mT at 0.15 and 0.3 mg/kg significantly ($P < .005$) increased platelet counts (Table 2), an observation consistent with the finding that some thiosemicarbazones mimic thrombopoietin.[72] In contrast to Dp44mT, 3-AP at its MTD (6 mg/kg) markedly and significantly ($P < .0001$) decreased animal weight, hemoglobin level, hematocrit, and erythrocyte and leukocyte cell counts (Table 2). These data suggested that though 3-AP markedly reduced tumor weight, at this dose the compound was systemically toxic.

Increased numbers of apoptotic cells in Dp44mT-treated tumor samples from mice and examination of apoptosis in cultured M109 cells

Using the in situ TUNEL assay, tumor samples from animals treated with Dp44mT (0.4 mg/kg) (Figure 4Bii) showed clear

Table 2. Weight loss and hematologic indices from mice treated with vehicle alone (control), Dp44mT, or 3-AP

		Dp44mT			
	Control	0.15 mg/kg	0.3 mg/kg	0.4 mg/kg	3-AP, 6 mg/kg
Body weight loss, g	0.8 ± 0.3	1.4 ± 0.2	1.3 ± 0.3	1.1 ± 0.2	5.3 ± 0.4
WBC count, $\times 10^9$/L	4.4 ± 0.4	4.2 ± 0.8	4.2 ± 0.4	3.9 ± 0.6	1.4 ± 0.3
RBC count, $\times 10^{12}$/L	9.1 ± 0.2	9.4 ± 0.1	8.9 ± 0.4	8.0 ± 0.6	6.1 ± 0.4
Hemoglobin level, g/L	137 ± 2	14.0 ± 2	133 ± 5	118 ± 8	86 ± 5
Hematocrit	0.46 ± 0.01	0.46 ± 0.01	0.40 ± 0.03	0.40 ± 0.01	0.28 ± 0.01
Platelet count, $\times 10^9$/L	788 ± 47	1047 ± 42	1019 ± 87	636 ± 88	976 ± 171

Female CD2FI mice, aged 8 to 10 weeks, underwent xenografting with M109 tumor cells. Dp44mT or 3-AP was administered intravenously twice daily for 5 consecutive days from day 4 after tumor implantation. Total body weight was measured on the 12th day after implantation (see "Materials and methods"). Mice were killed, and cardiac puncture was performed. Hematologic indices were measured as described in "Materials and methods." Results are mean ± SEM (3 separate experiments). WBC indicates white blood cell; RBC, red blood cell.

evidence of increased apoptotic cell death compared with vehicle-treated controls (Figure 4Bi). To further investigate the apoptotic pathways induced by Dp44mT, cultured M109 cells were incubated with the chelator for 24 hours and were analyzed for apoptosis or necrosis/late-stage apoptosis using Annexin V–FITC and PI staining, respectively. There was a dose-dependent elevation in apoptotic and necrotic/late-stage apoptosis cells after Dp44mT treatment (Figure 5A). Exposing cells to 1 μM Dp44mT caused a significant ($P < .05$) increase of apoptotic and necrotic/late-stage apoptotic cell numbers, and this increase in apoptotic cells peaked at 100 μM Dp44mT (Figure 5A). Using Dp44mT at 250 μM, apoptotic cell numbers decreased to 20% ± 2%, and the necrotic cell/late-stage apoptotic population increased to 42% ± 6%, suggesting dose-dependent cytotoxicity.

Induction of apoptosis by Dp44mT (1 μM) was also time dependent (Figure 5B). Incubation with 1 μM Dp44mT for 12 hours caused a significant ($P < .001$) increase in apoptotic cells (12% ± 2%). Hence, at 1 μM, Dp44mT markedly promoted ^{59}Fe release (Figure 3A,C), inhibited ^{59}Fe uptake (Figure 3B,D), and induced apoptotic cell death (Figure 5B). Therefore, 1 μM Dp44mT was assessed to further investigate the apoptotic pathways that were induced.

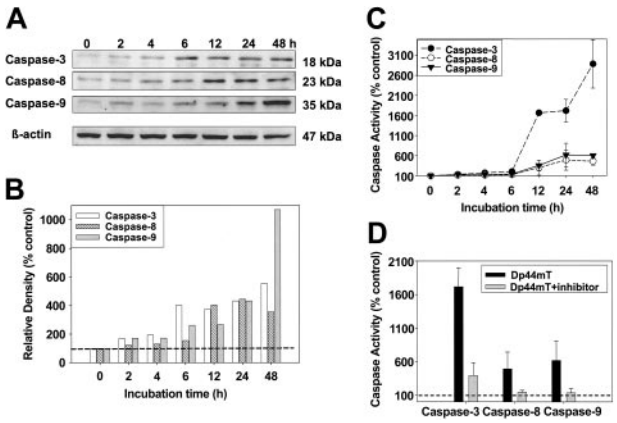

Figure 6. Effect of Dp44mT (1 μM) on the protein levels of active caspase-3, -8, and -9 and the activity of caspase-3, -8, and -9 in cultured M109 cells in the absence and presence of cell-permeable caspase inhibitors. (A) Caspase-3, -8, and -9 levels after Dp44mT treatment at the indicated times as detected by Western blotting (top blots). Anti–β-actin antibody was used to ensure equal protein loading (bottom blot). (B) Densitometric analysis of the expression of caspase-3, -8, and -9 as a function of time normalized to β-actin. (C) Caspase activity induced by Dp44mT (1 μM) at 0 to 48 hours was expressed as a percentage of the 0-hour time value. (D) Cell-permeable inhibitors of caspase-3, -8, or -9 at 1 μM prevented activation of these enzymes when incubated with Dp44mT (1 μM) for 48 hours. Results are mean ± SEM of 3 separate experiments. Horizontal dashed line indicates 100%.

Protein levels and activities of caspase-3, -8, and -9 in M109 cells after incubation with Dp44mT

To determine the role of caspase activation in Dp44mT-induced apoptosis in M109 cells, we examined protein levels of active caspase-3, -8, and -9 (Figure 6A-B) and their enzymatic activity (Figure 6C-D). Short incubations of 2 hours with Dp44mT (1 μM) increased the protein levels of caspase-3, -8, and -9 to 168%, 122%, and 171% of the control, respectively. Incubating M109 cells with Dp44mT (1 μM) for 6 hours resulted in an increase of caspase-3 to 400% of the control; increases of caspase-9 and caspase-8 were less marked at 280% and 150% of control, respectively (Figure 6A-B). A 12-hour incubation with Dp44mT resulted in caspase-8 protein levels of 400% of the control; levels for caspase-3 and -9 remained approximately the same as they were at 6 hours (380% and 280% of control, respectively). An incubation of 24 hours with Dp44mT increased the protein level of all caspases to approximately 4-fold that of control cells. After 48 hours, caspase-3, -8, and -9 levels were 5.5-, 3.4-, and more than 10-fold those of control cells, respectively (Figure 6A-B).

After incubation with Dp44mT (1 μM), the enzymatic activity of the caspases (Figure 6C) did not directly correlate with their protein levels (Figure 6A-B). The reasons for this could be due to differences in the sensitivity of the Western blot compared with the enzymatic activity assays and the different catalytic efficiencies of each caspase for its substrate. Caspase-3 activity increased most markedly after 6 hours, and this occurred in a time-dependent manner to 2900% of the control after 48 hours (Figure 6C). Caspase-8 and -9 activities increased to a far lesser extent, namely to 299% and 354% of the control after 12-hour incubation with Dp44mT (Figure 6C). The activity of these latter enzymes plateaued at 400% to 600% of the control after 24 hours (Figure 6C). Membrane-permeable inhibitors of each caspase at 1 μM reversed their activation when incubated with Dp44mT (1 μM) for 48 hours (Figure 6D), demonstrating the specificity of the activity.

Release of h-cytc from mitochondria into the cytosol after incubation with Dp44mT

Because of the importance of mitochondrial h-cytc release in apoptosis induction,[52,53] we investigated the effect of Dp44mT on this process using Western blot analysis (Figure 7A). Little h-cytc expression was evident in the cytosolic fractions of control M109 cells (ie, at 0 hours), with the greatest amount of the molecule found in the SMM at this time (Figure 7A). However, after 2-hour exposure to Dp44mT (1 μM), h-cytc was found in the cytosolic fraction of M109 cells, and there was a concomitant decrease in the SMM levels of this molecule (Figure 7A). The release of h-cytc into the cytosol plateaued after 4-hour incubation with Dp44mT and then decreased to that found in control cells after 24 and 48 hours. This increase in cytosolic h-cytc correlated with the loss from the SMM (Figure 7A). The near complete disappearance of

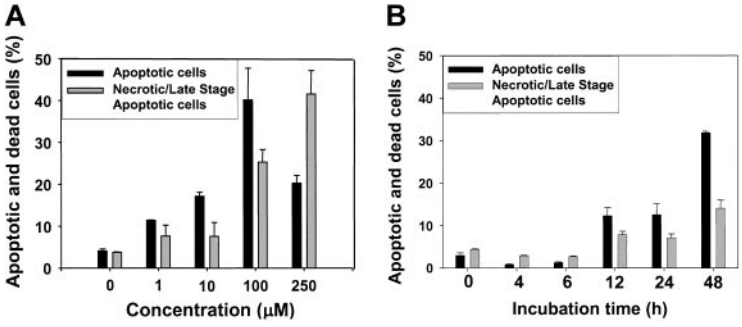

Figure 5. Effect of Dp44mT on M109 cellular apoptosis or necrosis/late-stage apoptosis. (A) Chelator concentration. M109 cells were incubated with Dp44mT at 0 to 250 μM for 24 hours at 37°C. Cellular apoptosis and necrosis/late-stage apoptosis were measured using Annexin V–FITC and PI staining, respectively (see "Materials and methods"). (B) Incubation time. M109 cells were treated with Dp44mT (1 μM) for various incubation times (0-48 hours). Cellular apoptosis and necrosis/late-stage apoptosis were measured as described for panel A. Data plotted are mean ± SEM of 3 separate experiments.

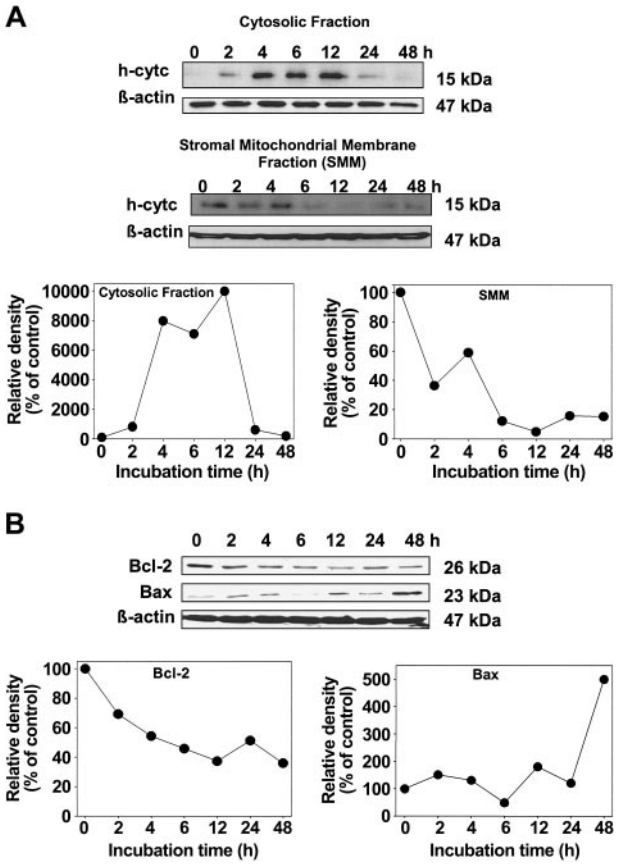

Figure 7. Effect of Dp44mT (1 μM) in cultured M109 cells on the holocytochrome *c* (h-cytc) levels in cytosolic and stromal-mitochondrial membrane (SMM) fractions and mitochondrial protein levels of Bcl-2 and Bax. (A) Cytosolic and SMM fractions of M109 cells were separated and subjected to Western blotting with anti–h-cytc antibody. The blot was reprobed with an anti–β-actin antibody to ensure equal protein loading. Densitometric analyses are shown beneath the blots; expression is normalized to β-actin. (B) Protein levels of Bcl-2 and Bax were determined through Western blotting using the SMM fraction of M109 cells after incubation with Dp44mT for 0 to 48 hours. Anti–β-actin antibody was used to ensure equal protein loading. Densitometric analysis is shown beneath each blot, where expression is normalized to β-actin. Results in panels A and B are representative of 3 experiments.

h-cytc from the cytosol at 24 and 48 hours may have been due to its release from cells or its degradation[53] (Figure 7A).

Bcl-2 and Bax expression in M109 cells after incubation with Dp44mT

Considering the roles of Bcl-2 and Bax in the mitochondrial pathway of apoptosis and their roles in h-cytc release,[52,61,62] the effect of Dp44mT (1 μM) on the SMM protein levels of these molecules was determined through Western blotting (Figure 7B). After incubation with Dp44mT (1 μM), the antiapoptotic molecule Bcl-2 gradually decreased as a function of time to 69% and 37% of the 0-hour time point after 2 hours and 48 hours, respectively (Figure 7B). Conversely, Bax expression increased markedly after a 48-hour incubation with Dp44mT, reaching 500% of that found at 0 hours (Figure 7B).

Intracellular ROS generation after incubation with Dp44mT

Cytotoxic mechanisms of some thiosemicarbazones involve redox cycling of their bound Fe and the generation of ROS.[7,9] Considering that oxidative stress readily induces h-cytc release from the mitochondrion (Figure 7A) and the imbalance of Bcl-2/Bax expression[70] (Figure 7B), we hypothesized that these responses were caused by ROS generated by the Dp44mT-Fe complex. To test this, intracellular ROS were measured by flow cytometry using the H_2DCF-DA probe, which becomes fluorescent when oxidized by O_2^-, H_2O_2, or HO−.[71]

Incubating M109 cells with Dp44mT (1 μM) increased the levels of oxidized probe as a function of time. After 2 hours, a 25% ± 10% increase in oxidized H_2DCF-DA fluorescence was found compared with the 0-hour time point, and this increased to 486% ± 96% after 48 hours. For comparison, a 10-minute incubation with the positive control, H_2O_2 (50 μM), increased fluorescence to 1312% ± 46% of that at the 0-hour time point.

Discussion

Increased resistance among some cancers to standard treatment has led to the investigation of new therapeutic strategies and to our examination of the activity of novel DpT analogs. The antiproliferative activity of some of these chelators (eg, Dp44mT) was greater than ligands previously characterized by others[25-28] and our laboratory.[7-9,23,24] Indeed, their activity was greater than that of 311 and 3-AP and was similar to that of doxorubicin (Table 1). Significantly, Dp44mT induced apoptosis and inhibited the growth of an aggressive lung carcinoma in vivo to 47% of control after only 5 days of treatment (Figure 4A). This pronounced activity was not accompanied by marked systemic hematologic indications of Fe deprivation or toxicity (Table 2), demonstrating its selectivity against tumor cells. Clearly, though these data suggest some selectivity in terms of chelator activity, more detailed studies are essential to assess the hematologic effects of the compounds and their influence on hematopoiesis using a range of time points.

The ability of DpT ligands to inhibit tumor cell growth (Table 1) was shown to correlate with their efficacy to induce ^{59}Fe release (Figure 3A) and to prevent ^{59}Fe uptake (Figure 3B). Indeed, the Fe chelation activities of Dp44mT, Dp4mT, Dp4eT, Dp4aT, and Dp4pT were similar to those found for 311 and greater than those mediated by DFO. The ability of these compounds to inhibit growth by binding Fe was evident by assessing Dp2mT. This ligand has a methyl group at the 2-position (Figure 1A) that prevented electron delocalization and inhibited metal binding (Figure 3A-B), and it resulted in no antiproliferative activity (Table 1). Collectively, these results demonstrate that ligands are potent chelators and that Fe chelation is involved in their ability to inhibit proliferation.

Our design rationale in creating these compounds has been based on the tridentate aroylhydrazone chelators characterized in our laboratory.[7-9,21-24,45,64] We recently showed that the analogous PKIH series of ligands (Figure 1) are tridentate.[74] Hence, based on the close structural similarities between the PKIH and DpT chelators (Figure 1), these latter ligands will be tridentate and will have a high affinity for Fe. Considering the formation constants for the related PCIH[74] and the solution and electrochemistry of the PKIH analogs,[73] it can be predicted that the DpT analogs will bind Fe(II) with high affinity. As with all Fe chelators, these ligands will, to some extent, also bind Zn(II) and Cu(II).[75] Because depletion of other metals, such as Zn(II), can also modulate apoptosis,[76] we cannot exclude that the apoptosis observed may be caused by chelators binding more than one type of metal ion.

Previous studies have shown that the ability of a chelator to bind cellular Fe leads to apoptosis.[24,26,49-51,56] If Fe chelators effect tumor cell death by engaging the apoptotic pathway, then regulating apoptosis becomes important for inhibiting cancer cell proliferation. Because Dp44mT was the most effective chelator yet screened for antitumor activity, it was crucial to assess its ability to induce apoptosis.

Considering the mode of apoptosis, the most striking increase in enzymatic activity was observed for caspase-3, which increased 29-fold compared with the control after a 48-hour incubation with Dp44mT (Figure 6C). In previous studies the chelators, hinokitiol,[77] and O-Trensox[26] also markedly increased caspase-3 activity, though other caspases were not assessed. The most detailed analysis of caspase activity after incubation with chelators has been provided for tachpyridine.[51] This latter investigation showed that caspase-9 activity was the most markedly induced, with less activity observed for caspase-3 and -8.[51] In contrast, in the current work, Dp44mT markedly increased caspase-3, with less activation of caspase-8 and -9 (Figure 6C), and these differences probably related to the different chemical properties of Dp44mT and tachpyridine.

To further investigate the mechanism of caspase activation, we examined the efflux of h-cytc from the mitochondrion (Figure 7A).[52] Incubation with Dp44mT for only 2 hours resulted in h-cytc release from the mitochondrion (Figure 7A), and this occurred at a similar time to activation of caspase-3, -8, and -9 (Figure 6A-C). This indicated that Dp44mT induced the mitochondrial pathway of apoptosis and accounted, at least in part, for the activation of caspases. Interestingly, h-cytc release within 2 hours (Figure 7A) coincided with the decrease in mitochondrial Bcl-2 expression (Figure 7B), which is involved in preventing h-cytc release.[52] However, a marked increase in Bax expression, which plays a role in h-cytc release and caspase activation,[52] was only observed after 48 hours (Figure 7B).[52] The imbalance of Bcl-2 and Bax expression might have resulted in mitochondrial h-cytc release, as found under other conditions.[52]

Considering h-cytc efflux from mitochondria, previous studies have demonstrated that oxidant stress is an inducer of its release as well as the down-regulation of Bcl-2, the up-regulation of proapoptotic proteins (eg, Bax), the activation of caspases, and the rupture of lysosomes.[70,78-82] Intriguingly, thiosemicarbazone-Fe complexes are markedly redox active.[7,9] Moreover, we have shown that the closely related group of PKIH chelators binds Fe(II) and mediates Fenton chemistry, resulting in DNA degradation.[73] In this investigation, an increase in ROS was detected after 2-hour incubation with Dp44mT, coinciding with h-cytc release (Figure 7A). Hence, as with the doxorubicin-Fe complex that redox cycles to generate radicals,[83] the Fe complex of Dp44mT is redox active, and this could play a role in its cytotoxic effects. Although our observations were consistent with a role of ROS in inducing h-cytc release, we cannot exclude other mechanisms. Indeed, one pronounced effect of Dp44mT was Fe chelation (Figure 3A-D). It is well known that ligands that do not generate ROS on binding Fe, such as DFO and 311,[7,9,64] induce apoptosis.[24,51] The fact that DFO induces h-cytc release[84] suggests Fe chelation alone may be sufficient to induce this effect.

In conclusion, the novel DpT analogs show potent and selective antiproliferative activity against cancer cells in vitro and in vivo. Indeed, Dp44mT is one of the most effective chelators developed in terms of its selective antitumor activity, and it warrants further vigorous investigation.

Acknowledgments

Children's Cancer Institute Australia for Medical Research (CCIA) is affiliated with the University of New South Wales and Sydney Children's Hospital. We thank Dr J. Kwok and Mr Ian Napier of the Iron Metabolism and Chelation Program (IMCP) for their comments on the manuscript before submission. We give special thanks to Dr Richard Lock and Dr Karen MacKenzie for their careful assessment of this manuscript. We also acknowledge Dr Ralph Watts (IMCP) for his expert assistance with the figures.

References

1. Le NTV, Richardson DR. The role of iron in cell cycle progression and the proliferation of neoplastic cells. Biochim Biophys Acta. 2002;1603: 31-46.
2. Blatt J, Stitely S. Antineuroblastoma activity of desferrioxamine in human cell lines. Cancer Res. 1987;47:1749-1750.
3. Estrov Z, Tawa A, Wang X-H, et al. In vivo and in vitro effects of desferrioxamine in neonatal acute leukemia. Blood. 1987;69:757-761.
4. Becton DL, Bryles P. Deferoxamine inhibition of human neuroblastoma viability and proliferation. Cancer Res. 1988;48:7189-7192.
5. Donfrancesco A, Deb G, Dominici C, et al. Effects of a single course of deferoxamine in neuroblastoma patients. Cancer Res. 1990;50:4929-4930.
6. Finch RA, Liu M-C, Grill SP, et al. Triapine (3-aminopyridine-2-carboxaldehyde-thiosemicarbazone): a potent inhibitor of ribonucleotide reductase activity with broad spectrum antitumor activity. Biochem Pharmacol. 2000;59:983-991.
7. Lovejoy DB, Richardson DR. Novel "hybrid" iron chelators derived from aroylhydrazones and thiosemicarbazones demonstrate high anti-proliferative activity that is selective for tumor cells. Blood. 2002;100:666-676.
8. Becker E, Lovejoy DB, Greer JM, Watts RN, Richardson DR. Novel aroylhydrazone iron chelators differ in their iron chelation efficacy and antiproliferative activity: identification of a new class of potential anti-proliferative agents. Br J Pharmacol. 2003;138:819-830.
9. Chaston TB, Lovejoy DB, Watts RN, Richardson DR. Examination of the anti-proliferative activity of iron chelators: multiple cellular targets and the different mechanism of action of triapine compared to desferrioxamine and the potent PIH analogue 311. Clin Cancer Res. 2003;9:402-414.
10. Hershko C. Control of disease by selective iron depletion: a novel therapeutic strategy utilizing iron chelators. Baillière's Clin Haematol. 1994;7: 965-1000.
11. Lovejoy DB, Richardson DR. Iron chelators as anti-neoplastic agents: current developments and promise of the PIH class of chelators. Curr Med Chem. 2003;10:1065-1078.
12. Larrick JW, Cresswell P. Modulation of cell surface iron transferrin receptors by cellular density and state of activation. J Supramol Struct. 1979; 11:579-586.
13. Richardson DR, Baker E. The uptake of iron and transferrin by the human melanoma cell. Biochim Biophys Acta. 1990;1053:1-12.
14. Richardson DR, Baker E. Two mechanisms of iron uptake from transferrin by melanoma cells: the effect of desferrioxamine and ferric ammonium citrate. J Biol Chem. 1992;267:13972-13979.
15. Trinder D, Zak O, Aisen P. Transferrin receptor-independent uptake of diferric transferrin by human hepatoma cells with antisense inhibition of receptor expression. Hepatology. 1996;23:1512-1520.
16. Thelander L, Reichard P. The reduction of ribonucleotides. Annu Rev Biochem. 1979;48:133-158.
17. Nyholm S, Mann GJ, Johansson AG, Bergeron RJ, Graslund A, Thelander L. Role of ribonucleotide reductase in inhibition of mammalian cell growth by potent iron chelators. J Biol Chem. 1993;268:26200-26205.
18. Cooper CE, Lynagh GR, Hoyes KP, Hider RC, Cammack R, Porter JB. The relationship of intracellular iron chelation to the inhibition and regeneration of human ribonucleotide reductase. J Biol Chem. 1996;271:20291-20299.
19. Witt L, Yap T, Blakely RL. Regulation of ribonucleotide reductase activity and its possible exploitation in chemotherapy. Adv Enzyme Regul. 1979; 17:157-171.
20. Takeda E, Weber G. Role of ribonucleotide reductase in expression in the neoplastic program. Life Sci. 1981;28:1007-1014.
21. Green DA, Antholine WE, Richardson DR, Chitambar CR. Ribonucleotide reductase as a preferential target for the inhibition of leukemic cell growth by 311, a novel iron chelator of the pyridoxal isonicotinoyl hydrazone class. Clin Cancer Res. 2001;7:3574-3579.
22. Richardson DR, Ponka P, Baker E. The effect of the iron(III) chelator, desferrioxamine, on iron and transferrin uptake by the human malignant melanoma cell. Cancer Res. 1994;54:685-689.
23. Richardson DR, Tran EH, Ponka P. The potential of iron chelators of the pyridoxal isonicotinoyl hydrazone class as effective anti-proliferative agents. Blood. 1995;86:4295-4306.
24. Richardson DR, Milnes K. The potential of iron chelators of the pyridoxal isonicotinoyl hydrazone class as effective antiproliferative agents, II: the mechanism of action of ligands derived from salicylaldehyde benzoyl hydrazone and 2-hydroxy-1-naphthylaldehyde benzoyl hydrazone. Blood. 1997;89:3025-3038.
25. Torti SV, Torti FM, Whitman SP, Brechbiel MW, Park G, Planalp RP. Tumor cell cytotoxicity of a novel metal chelator. Blood. 1998;92:1384-1389.
26. Rakba N, Loyer P, Gilot D, et al. Anti-proliferative and apoptotic effects of O-Trensox, a new synthetic iron chelator, on differentiated human hepatoma cell lines. Carcinogenesis. 2000;21:943-951.
27. Simonart T, Degraef C, Andrei G, et al. Iron chelators inhibit the growth and induce the apoptosis of

Kaposi's sarcoma cells and of their putative endothelial precursors. J Invest Dermatol. 2000;115:893-900.

28. Kicic A, Chua AC, Baker B. Desferrithiocin is a more potent antineoplastic agent than desferrioxamine. Br J Pharmacol. 2002;135:1393-1402.
29. Wang F, Elliott RL, Head JF. Inhibitory effect of deferoxamine mesylate and low iron diet on the 13762NF rat mammary adenocarcinoma. Anticancer Res. 1999;19:445-450.
30. Kemp JD, Cardillo T, Stewart BC, et al. Inhibition of lymphoma growth in vivo by combined treatment with hydroxyethyl starch deferoxamine conjugate and IgG monoclonal antibodies against the transferrin receptor. Cancer Res. 1995;55:3817-3824.
31. Dezza L, Cazzola M, Danova M, et al. Effects of desferrioxamine on normal and leukemic human hematopoietic cell growth: in vitro and in vivo studies. Leukemia. 1989;3:104-107.
32. Donfrancesco A, Deb G, Dominici C, et al. Deferoxamine, cyclophosphamide, etoposide, carboplatin, and thiotepa (D-CECat): a new cytoreductive chelation-chemotherapy regimen in patients with advanced neuroblastoma. Am J Clin Oncol. 1992;15:319-322.
33. Donfrancesco A, De Bernardi B, Carli M, et al. Deferoxamine (D) followed by cytoxan (C), etoposide (E), carboplatin (Ca), thio-TEPA (T), induction regimen in advanced neuroblastoma. Eur J Cancer. 1995;31A:612-615.
34. Giles FJ, Fracasso PM, Kantarjian HM, et al. Phase I and pharmacodynamic study of Triapine, a novel ribonucleotide reductase inhibitor, in patients with advanced leukemia. Leuk Res. 2003;27:1077-1083.
35. Feun L, Modiano M, Lee K, et al. Phase I and pharmacokinetic study of 3-aminopyridine-2-carboxaldehyde thiosemicarbazone (3-AP) using a single intravenous dose schedule. Cancer Chemother Pharmacol. 2002;50:223-229.
36. Krakoff IH, Etcubanas E, Tan C, Mayer K, Bethune V, Burchenai JH. Clinical trial of 5-hydroxypicolinaldehyde thiosemicarbazone (5-HP: NSC-107392), with special reference to its Fe chelating properties. Cancer Chemother Rep. 1974;53:207-212.
37. Richardson DR. Iron chelators as effective antiproliferative agents. Can J Physiol Pharmacol. 1997;75:1164-1180.
38. Bottomley SS, Wolfe LC, Bridges KR. Iron metabolism in K562 erythroleukemia cells. J Biol Chem. 1985;260:6811-6815.
39. Blatt J. Deferoxamine in children with recurrent neuroblastoma. Anticancer Res. 1994;14:2109-2112.
40. Selig RA, White L, Gramacho C, Sterlinglevis K, Fraser IW, Naidoo D. Failure of iron chelators to reduce tumor growth in human neuroblastoma xenografts. Cancer Res. 1998;58:473-478.
41. Ponka P, Borova J, Neuwirt J, Fuchs O. Mobilization of iron from reticulocytes: identification of pyridoxal isonicotinoyl hydrazone as a new iron chelating agent. FEBS Lett. 1997;97:317-321.
42. Ponka P, Borova J, Neuwirt J, Fuchs O, Necas E. A study of intracellular iron metabolism using pyridoxal isonicotinoyl hydrazone and other synthetic chelating agents. Biochim Biophys Acta. 1979;586:278-297.
43. Hershko C, Avramovici-Grisaru S, Link G, Gelfand L, Sarel S. Mechanism of in vivo iron chelation by pyridoxal isonicotinoyl hydrazone and other imino derivatives of pyridoxal. J Lab Clin Med. 1981;98:99-108.
44. Brittenham GM. Pyridoxal isonicotinoyl hydrazone: an effective iron-chelator after oral administration. Semin Hematol. 1990;27:112-116.
45. Darnell G, Richardson DR. The potential of analogues of the pyridoxal isonicotinoyl hydrazone class as effective anti-proliferative agents, III: the effect of the ligands on molecular targets involved in proliferation. Blood. 1999;94:781-792.
46. Gao J, Richardson DR. The potential of iron chelators of the pyridoxal isonicotinoyl hydrazone class as effective anti-proliferative agents, IV: the mechanisms involved in inhibiting cell cycle progression. Blood. 2001;98:842-850.
47. Le NTV, Richardson DR. Potent iron chelators increase the mRNA levels of the universal cyclin-dependent kinase inhibitor, $p21^{WAF1/CIP1}$, but paradoxically inhibit translation: a potential mechanism of cell cycle dysregulation. Carcinogenesis. 2003;24:1045-1058.
48. Liang SX, Richardson DR. The effect of potent iron chelators on the regulation of p53: examination of the expression, localization, and DNA-binding activity of p53 and the transactivation of *WAF1.* Carcinogenesis. 2003;24:1601-1614.
49. Hileti D, Panayiotidis P, Hoffbrand AV. Iron chelators induce apoptosis in proliferating cells. Br J Haematol. 1995;89:181-187.
50. Abeysinghe RD, Greene BT, Haynes R, et al. p53-independent apoptosis mediated by tachpyridine, an anti-cancer iron chelator. Carcinogenesis. 2001;22:1607-1614.
51. Greene BT, Thorburn J, Willingham MC, et al. Activation of caspase pathways during iron chelator–mediated apoptosis. J Biol Chem. 2002;277:25568-25575.
52. Lim MLR, Lum M-G, Hansen TM, Roucou X, Nagley P. On the release of cytochrome c from mitochondria during cell death signaling. J Biomed Sci. 2002;9:488-506.
53. Jemmerson R, LaPlante B, Treeful A. Release of intact, monomeric cytochrome c from apoptotic and necrotic cells. Cell Death Differ. 2002;9:538-548.
54. Chandra J, Samali A, Orrenius S. Triggering and modulation of apoptosis by oxidative stress. Free Radic Biol Med. 2000;29:323-333.
55. Kaufmann SH, Earnshaw WC. Induction of apoptosis by cancer chemotherapy. Exp Cell Res. 2000;256:42-49.
56. Ul-Haq RU, Wereley JP, Chitambar CR. Induction of apoptosis by iron deprivation in human leukemic CCRF-CEM cells. Exp Hematol. 1995;23:428-432.
57. Cohen GM. Caspases: the executioners of apoptosis. Biochem J. 1997;326:1-16.
58. Earnshaw WC, Martins LM, Kaufmann SH. Mammalian caspases: structure, activation, substrates, and functions during apoptosis. Annu Rev Biochem. 1999;68:383-424.
59. Green DR. Apoptotic pathways: the roads to ruin. Cell. 1998;94:695-698.
60. Budihardjo I, Oliver H, Lutter M, Luo X, Wang X. Biochemical pathways of caspase activation during apoptosis. Annu Rev Cell Dev Biol. 1999;15:269-290.
61. Kluck RM, Bossy-Wetzel E, Green DR, Newmeyer DD. The release of cytochrome c from mitochondria: a primary site for Bcl-2 regulation of apoptosis. Science. 1997;275:1132-1136.
62. Jurgensmeier JM, Xie Z, Deveraux Q, Ellerby L, Bredesen D, Reed JC. Bax directly induces release of cytochrome c from isolated mitochondria. Proc Natl Acad Sci U S A. 1998;95:4997-5002.
63. Finch RA, Liu M-C, Cory AH, Cory JG, Sartorelli AC. Triapine (3-aminopyridine-2-carboxaldehyde thiosemicarbazone; 3-AP): an inhibitor of ribonucleotide reductase with antineoplastic activity. Adv Enzyme Regul. 1999;39:3-12.
64. Richardson DR, Bernhardt PV. Crystal and molecular structure of 2-hydroxy-1-naphthaldehyde isonicotinoyl hydrazone (NIH) and its iron(III) complex: an iron chelator with anti-tumour activity. J Biol Inorg Chem. 1999;4:266-273.
65. Bacchi A, Carcelli M, Costa M, Pelagatti P, Pelizzi C, Pelizzi G. Versatile ligand behaviour of phenyl 2-pyridyl ketone benzoyl hydrazone in palladium(II) complexes. J Chem Soc Dalton Trans. 1996;22:4239-4244.
66. Karin M, Mintz B. Receptor-mediated endocytosis of transferrin in totipotent mouse teratocarcinoma cells. J Biol Chem. 1981;256:3245-3252.
67. Gavrieli Y, Sherman Y, Ben-Sasson SA. Identification of programmed cell death in situ via specific labeling of nuclear DNA fragmentation. J Cell Biol. 1992;119:493-501.
68. Yuan J, Murrell GA, Wei AQ, Wang MX. Apoptosis in rotator cuff tendonopathy. J Orthop Res. 2002;20:1372-1379.
69. Vermes I, Haanen C, Steffens-Nakken H, Reutelingsperger C. A novel assay for apoptosis: flow cytometric detection of phosphatidylserine expression on early apoptotic cells using fluorescein labelled Annexin V. J Immunol Methods. 1995;184:39-51.
70. Yuan J, Murrell GA, Trickett A, Wang MX. Involvement of cytochrome c release and caspase-3 activation in the oxidative stress-induced apoptosis in human tendon fibroblasts. Biochim Biophys Acta. 2003;1641:35-41.
71. Wang M, Wei AQ, Yuan J, Trickett A, Knoops B, Murrell GAC. Expression and regulation of peroxiredoxin 5 in human osteoarthritis. FEBS Lett. 2002;532:359-362.
72. Duffy KJ, Shaw AN, Delorme E, et al. Identification of a pharmacophore for thrombopoietic activity of small, non-peptidyl molecules, I: discovery and optimization of salicylaldehyde thiosemicarbazone thrombopoietin mimics. J Med Chem. 2002;45:3573-3575.
73. Ido Y, Muto N, Inada A, et al. Induction of apoptosis by hinokitiol, a potent iron chelator, in teratocarcinoma F9 cells is mediated through the activation of caspase-3. Cell Prolif. 1999;32:63-73.
74. Bernhardt PV, Caldwell LM, Chaston TB, Chin P, Richardson DR. Cytotoxic iron chelators: characterization of the structure, solution chemistry and redox activity of the di-2-pyridylketone isonicotinoyl hydrazone (HPKIH) analogues. J Biol Inorg Chem. 2003;8:866-880.
75. Armstrong CM, Bernhardt PV, Chin P, Richardson DR. Structural variations and formation constants of first row transition metal complexes of biologically active aroylhydrazones. Eur J Inorg Chem. 2003;1145-1156.
76. Irving H, Williams RJP. Order of stability of metal complexes. Nature. 1948;162:746-747.
77. Sunderman FW. The influence of zinc on apoptosis. Ann Clin Lab Sci. 1995;25:134-142.
78. Cook SA, Sugden PH, Clerk A. Regulation of Bcl-2 family proteins during development and in response to oxidative stress in cardiac myocytes: association with changes in mitochondrial membrane potential. Circ Res. 1999;85:940-949.
79. Atlante A, Calissano P, Bobba A, Azzariti A, Marra E, Passarella S. Cytochrome c is released from mitochondria in a reactive oxygen species (ROS)–dependent fashion and can operate as a ROS scavenger and as a respiratory substrate in cerebellar neurons undergoing excitotoxic death. J Biol Chem. 2000;275:37159-37166.
80. Takeyama N, Miki S, Hirakawa A, Tanaka T. Role of the mitochondrial permeability transition and cytochrome c release in hydrogen peroxide-induced apoptosis. Exp Cell Res. 2002;274:16-24.
81. Ueda S, Nakamura H, Masutani H, et al. Redox regulation of caspase-3(-like) protease activity: regulatory roles of thioredoxin and cytochrome c. J Immunol. 1998;161:6689-6695.
82. Zhao M, Antunes F, Eaton JW, Brunk UT. Lysosomal enzymes promote mitochondrial oxidant production, cytochrome c release and apoptosis. Eur J Biochem. 2003;270:3778-3786.
83. Muindi JRF, Sinha BK, Myers CE. Hydroxyl radical production and DNA damage induced by anthracycline iron complex. FEBS Lett. 1984;172:226-230.
84. Kim BS, Yoon KH, Oh HM, et al. Involvement of p38 MAP kinase during iron chelator-mediated apoptotic cell death. Cell Immunol. 2002;220:96-106.